



CFD Letters

Journal homepage:
https://semarakilmu.com.my/journals/index.php/CFD_Letters/index
 ISSN: 2180-1363



Impact of Wind-Assisted Technologies on Resistance and Stability of Commercial Ship

Aditya Agung Haripriyono¹, Yaseen Adnan Ahmed^{1,*}, Mohammed Abdul Hannan²

¹ Department of Aeronautical, Automotive and Offshore Engineering, Fakulti Kejuruteraan Mekanikal, Universiti Teknologi Malaysia, 81310 Skudai, Johor, Malaysia

² Faculty of Science, Agriculture and Engineering, Newcastle University, United Kingdom (Singapore campus)

ARTICLE INFO

Article history:

Received 26 July 2021

Received in revised form 10 October 2021

Accepted 11 October 2021

Available online 21 November 2021

Keywords:

Wing-sail; Fowler flap; CFD; Fuel saving;
CO₂ emission; Stability

ABSTRACT

The use of fossil fuels on commercial ships significantly contributes to the increase of carbon dioxide emission, and adaptation of renewable energy can help control that emission efficiently. Historically, the extraction of wind energy is found to be the best renewable energy solution for commercial ships; and recently, with renewed interest in this area, various wind energy extraction devices are proposed in the literature. This study investigates the effectiveness of one such technology, wing-sail, on a tanker ship. The NACA 4412 series is adopted to design the sail in this regard, and a fowler flap is added to aid the sail in low wind speed. ANSYS Fluent is used to carry out this CFD simulation-based study. The effects of onboard wing-sails under various apparent wind angles, wind speeds, and wing-sail orientations have been examined. The impact of wing-sail on the stability of the ship is also analyzed. It is concluded that the ship can save fuel and reduce carbon dioxide emissions by 1.8% to 2.4% while using the wing-sail with the aid of a fowler flap. Also, this combination of wing-sail with the fowler flap is found to be the best in providing extra thrust for commercial ships without significantly sacrificing its stability.

1. Introduction

Nowadays, the world is facing environmental crises, such as global warming, limited fossil fuel, and a high emission trend every year. All of these issues are directly related to transportation systems, in which marine transportation contributes to around 25% of all fuel consumption globally. Moreover, the highest contribution to CO₂ emission is coming from commercial ships with total emissions of approximately 80 percent [1, 2]. To curb these issues, the best possible way is to find alternatives to fossil fuels, and this could be done by harnessing renewable energies. Several published works have mentioned that extracting wind energy is an appropriate solution for renewable energy comparing to other available options. Because the ocean environments always tend to be windy, wind energy is expected to be found in the ocean all the time. Therefore, harnessing this energy could be the easiest solution to reduce commercial ship dependence on fossil energy [3].

* Corresponding author.

E-mail address: yaseen@mail.fkm.utm.my (Yaseen Adnan Ahmed)

<https://doi.org/10.37934/cfdl.13.11.95115>

In this regard, this paper investigates the effectiveness of utilizing wing-sail technology adapted from NACA series 4412 together with the fowler flap for a commercial ship. Additionally, this research highlights the advantages of using this technology in terms of providing additional ship thrust, which results in burning less fuel, and, thus less CO₂ emission. Different wind speeds, wind directions, and sail orientations are taken into account while using wing-sails to know the overall effect on ship performance. Moreover, as any newly installed wing-sail could drag the ship's center of gravity upward, it might affect the ship's intact stability while sailing in a windy area [4, 5]. Therefore, a ship using wing-sail has been investigated to satisfy the metacentric height and weather criteria at high wind speed [6]. On the other hand, previous researchers only focused on investigating the sails without considering the effect of the ship superstructure, which interrupts the flow. Thus, using ANSYS Fluent, the whole ship with the superstructure and the wing-sails are modeled and simulated for different wind directions and sail orientations.

The main objective of this study is to identify the effectiveness of using wing-sail for a commercial ship. In this regard, the suitability of utilizing the wing-sail and fowler flap-assisted wing-sail are investigated under low wind conditions, and the best wing-sail type is selected. After installing the wing-sails, the ship's intact stability is also determined and compared with the original ship. The results presented in this paper will thus allow us to choose an optimal wing-sail for a commercial ship, without much sacrificing the ship stability.

1.1 Literature Review

1.1.1 Technology of wing-sail

Many previous studies have investigated the characteristics of aerodynamic of rigid sails [7, 8]. In the beginning, the traditional vessel has a non-symmetrical arc-shaped sail with soft sail material. Indeed, this profile has good aerodynamic performance [8, 9]. However, a previous study explained that the rigid sail has a higher lift coefficient than the soft sail [7]. Besides, after the oil crisis, the rigid sail has been proposed to be applied for several ships, in which ships with rigid sail succeeded in reducing the fuel consumption by around 10% [7]. Recent studies stated that optimizing the hard wing-sail in sail-assisted vessels could improve energy efficiency [8]. Hence, this research determines the effectiveness of wing-sail technologies, such as fowler flap assisted sail for a 108 meters Tanker. CFD simulation is done for this purpose. Unlike others, to make the simulation more realistic, this research considers the whole hull with superstructure and a series of sails attached to itself within the computational domain to calculate the lift and drag forces more accurately. Later, to analyze the impact of wing sail on ship stability, a strategy proposed by Amin *et al.*, [6] is used for this tanker ship. Thus, this paper is unique in terms of considering a fowler flap assisted sail for the first time for a commercial ship and also considering the whole ship, its superstructure, and the sails together in the computational domain for a combined effect.

So far, many applications of wing-sail technologies were adapted from the NACA series, in which most studies were adapted from four-digit code NACA airfoil sections. Moreover, wing-sail with airfoil cross-section of the NACA-4412 provided better aerodynamics performances [6]. Nowadays, the studies of wing-sail technologies have begun to look upon aviation technologies in order to make the wing-sail design innovative with an adaptation of the aero plane's wing flap. There are different types of wing flaps available, which are developed by many researchers. The most profound type of flap used in aviation is the fowler flap [10]. The fowler flap is a split flap that slides rearwards on airplane wings. Therefore, the flap shifting backward results in curvature on the wing which helps to significantly increase lift [11] and a slight increase in drag [12]. Thus, this study considers both sail

and flap-assisted sail for the feasibility study of a commercial ship. The cross-section of each type is shown in Figure 1.



Fig. 1. Cross-section of NACA-4412 (a) without flap and (b) with flap

1.1.2 Numerical analysis, grid Independence, and validation

In recent times, many researchers have investigated the fluid flow problems acting on foils. In addition, many previous papers reviewed that Computational Fluid Dynamics (CFD) simulation is the best way to get results that match closely to the experimental fluid dynamics (EFD). The CFD is a fluid mechanics branch that uses numerical analysis and data structures to analyze and solve fluid flow problems [13, 14]. Also, the SST $k-\omega$ (omega) turbulence model is a two-Equations eddy-viscosity model used for many aerodynamic applications [15]. Thus, we utilize ANSYS Fluent platform for CFD simulations and the SST $k-\omega$ (omega) turbulence model within it to get a better result.

Furthermore, the grid independence study is also conducted for the CFD simulation to determine the 'correct' mesh size [16]. This grid independence study is carried out to guarantee that the computational results are unaffected by element size resolution [17]. Before we did a simulation ship with wing-sail, we did obtain grid independence from the wing-sail simulation. the first thing, we make model wing-sail NACA S 4412 full scale 1:1 and did configuration shown in below. Figure 2 shows the meshed the wing-sail that was used in ANSYS Fluent platform.

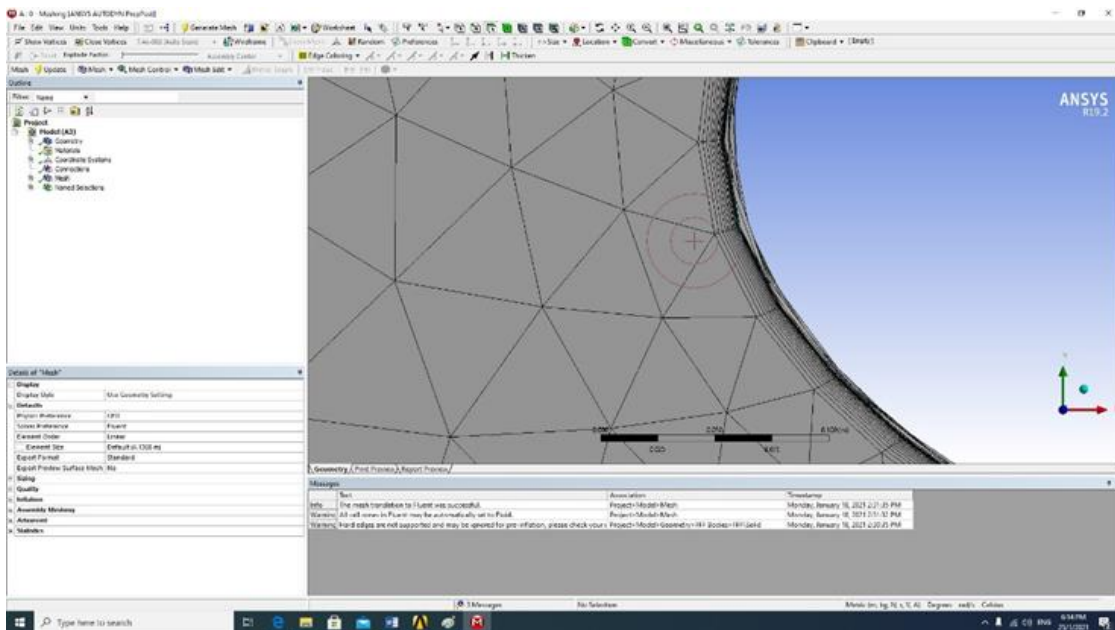


Fig. 2. Mesh tetrahedron wing-sail NACA S-4412

This project had tested eight different elements to obtain grid independence. Grid independence results should be determined from the results of the convergence graph and have a running computation timing that is not too long. In Figure 3, it can be seen that in this study the experimental results are considered for the lift coefficient, CL value. The element value taken is 1110997 because it gives the CL which is closer to the previous experiment's validation results and has a short solving time.

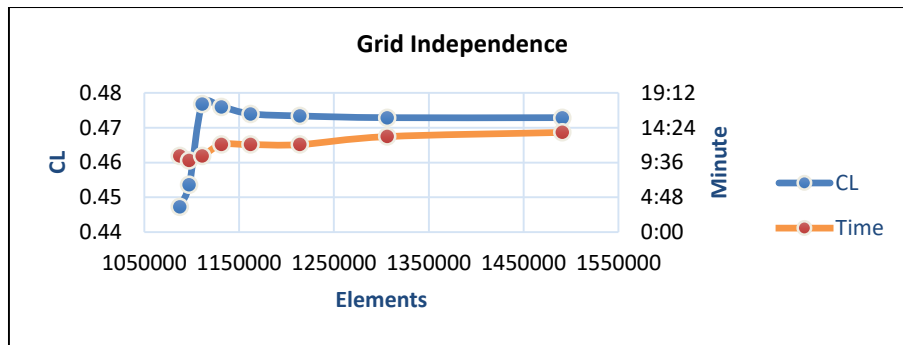


Fig. 3. Graph Grid Independence

After carrying out the independent grid study, furthermore, we simulated wing-sail with 18 different angles of attack. We continued with validation CL value compared with data from Airfoil tools with Reynolds number 1×10^6 , and the results are in Figure 4.

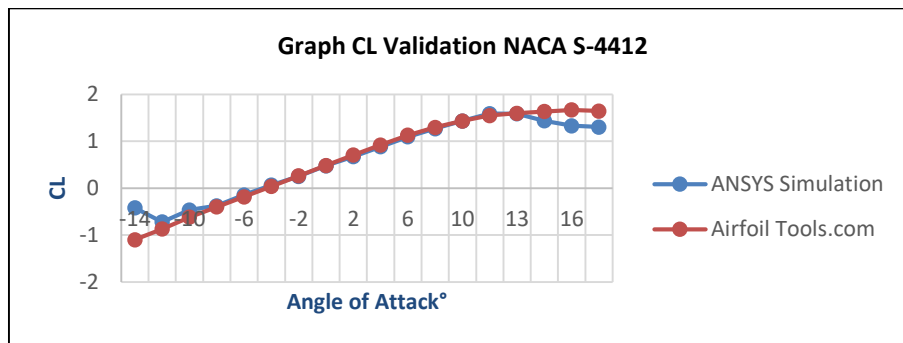


Fig. 4. Graph validation of CL from simulation CFD compare with Airfoiltools

2. Methodology

2.1 Subject Ship Selection

An oil tanker of length 108m shown in Figure 5 is chosen as a subject ship in this study. Its lines plan, and other principal dimensions are mentioned in Table 1, respectively. Maintaining the lines plan and the principal dimensions, a 3D model has been created with a scale of 1:1 in SOLIDWORKS, and four wing-sails are added into it. Later, the model is imported to ANSYS Fluent workbench for further investigation.



Fig. 5. Ship tanker 108m building on BATAMEC Shipyard [18]

Table 1
 Principal dimension

Parameter	Unit	Value
Deadweight	DWT	6500
Length Overall	m	108
Breadth (Moulded)	m	19.2
Depth (Moulded)	m	9.3
Draft	m	6.00
Block Coefficient	-	0.781

2.2 Route Selection

An oil tanker below 50,000 DWT is usually considered to be in the coastal tanker-size category. Thus, considering the subject ship's small tank size, the route is selected as port-to-port. This involves a more or less regular service between two ports, which has unidirectional freight flows involving empty backhauls and ships sailing with routes moving back and forth [19]. This research considers one trade route in West Indonesia from Meulaboh port to Teluk Bayur port. The detailed routes and voyage illustrations are shown in Table 2 and Figure 6.

Table 2
 Route outline (Meulaboh -Teluk Bayur)

Description	Unit	Value
Distance Travelled	Nautical Miles	428.2
Passage Time	hour	36
Apparent Wind Speed	m/s	4.378
Temperature	° Celsius	30

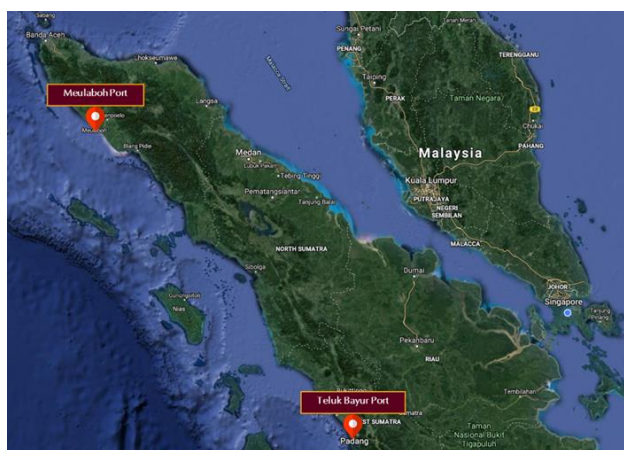


Fig. 1. Route Outline

2.3 Coordinate System and Force Analysis

This section defines some essential reference frames to describe the placements and orientations of wing- sail and wind directions while the ship is sailing. When a ship is running by following X direction, the aerodynamic forces acting on the sail model are decomposed as forces in different directions with the wind-axis coordinate system. Moreover, the aerodynamic wind forces acting on the sail could be decomposed as drag force F_D with the same direction as airflow, lifting force F_L perpendicular to the airflow. Symbols X and Y represent the traveling direction and transverse direction for the ship, respectively. The forces acting on the wing sail are shown in Figure 7.

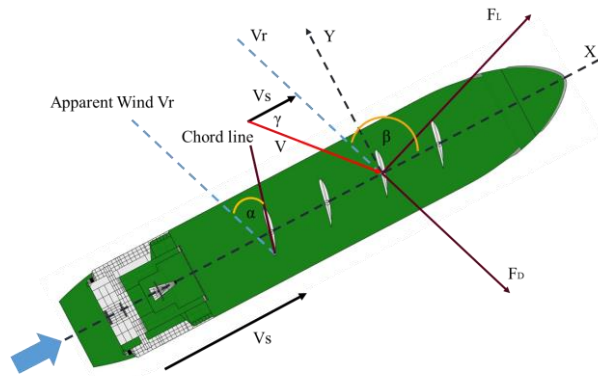


Fig. 2. The coordinate system of wing-sail and ship

Additionally, the 'point of sail' is fundamental for basic sailing as it defines a ship's direction of travel related to the wind direction over the sea surface [20]. The 'point of sail' adopted in this research is shown in Figure 8, which is divided into the following four categories with the wind blows from the port side:

- (a) Close hauled: When the apparent wind blowing tilting from the front of the ship with the wind angle fixed at 45° .
- (b) Beam reach: When the apparent wind blowing from the side of the ship with an apparent wind angle fixed at 90° .
- (c) Broad reach: When the apparent wind blowing between beam wind and downwind running with an apparent wind angle between 90° and 180° .
- (d) Running downwind: When the apparent wind blowing in the stern of the ship, with a fixed angle of 180° .

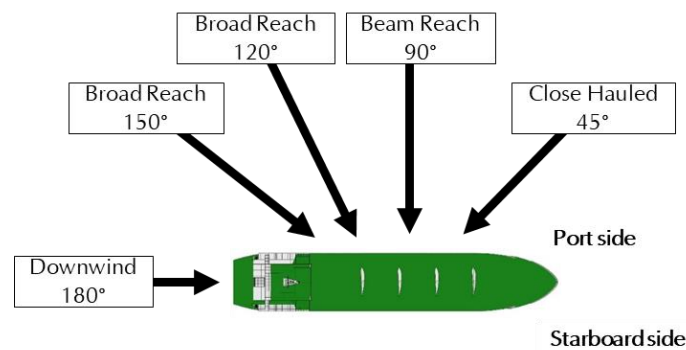


Fig. 3. Point of sail

2.4 Configuration and Simulation on ANSYS Fluent

In this step, the wing sail is analyzed for different wind configurations on a CFD software ANSYS 19.2 Fluent. The CFD modeling process usually starts with the definition of the geometry to be simulated. The geometry is then imported to a computational domain and discretized into computational grids (mesh).

In this simulation, we used a full-scale tanker ship, a 108-meter model, and a single-phase analysis. It means we have considered the above-water part of the ship with its superstructure and four-wing sails. The reason behind considering this single-phase analysis (only blow the wind) is the limited performance of hardware to run ANSYS 19.2.

Additionally, in this simulation, the viscous setup uses the SST $k - \omega$ (omega) model for turbulence. This is because the turbulence model has an advantage for addressing some specific flaws of the base model, and it has been used for many aerodynamic applications [21, 22]. In addition, it is the most commonly used model in the industry due to its high accuracy to expense ratio. This model selection is then followed by defining the boundary conditions for the fluid domain for this the problem needs to be solved. Once the simulation environment has been set up, the solution is obtained by running an appropriate numerical algorithm. Finally, the results are analyzed in the post-processing phase.

Figure 9 shows the configuration domain in ANSYS-Fluent simulation. We have used a similar domain for different variations, such as variation in wing sail type, variation in wing sail orientations, a constant apparent wind speed of 4.378 m/s, and variation in the apparent wind angles. The setup and configuration ANSYS-Fluent simulation are shown in table 3.

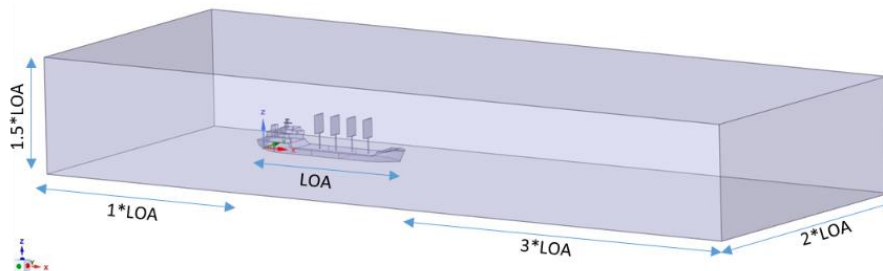


Fig. 4. Domain on ANSYS Fluent

Table 3
 Setup and configuration in ANSYS 19.2 Fluent

Index	Value	Annotation
Apparent Wind Angle	Hauled closed wind (45°)	AWA°
	Beam wind (90°)	
	Broad reach wind (120°)	
	Broad reach wind (150°)	
	Downwind running (180°)	
Temperature	30 °C	Temperature in Celsius
ρ	1.164 kg/m ³	Density of Air
μ	1.872E-05 kg/m s	Dynamic viscosity Air
ν	1.608E-05 m ² /s	Kinematic viscosity Air
Apparent wind speed	4.378 m/s	Velocity (AWS)
y^+	0.3	
Viscous model	SST k-omega	
Mesh	Tetrahedron	

The output of the ANSYS Fluent simulation gives the value of Lift force (F_L) and Drag force (F_D) for each different setup. After that, we have calculated the value of Thrust (Driving Force or Normal force) and also Drift (Lateral Force or sideways force) by using Eq. (1) and Eq. (2) [23], respectively.

$$T = F_L \cos \alpha + F_D \sin \alpha \quad (1)$$

$$H = F_D \cos \alpha - F_L \sin \alpha \quad (2)$$

Where, T is thrust (N), H is sideways force (N), α is apparent wind angle (degree), F_L is lift force (N), and F_D is drag force (N).

2.5 Total Fuel Saving & Total CO₂ Emission

After completing the determination of ship thrust, total fuel consumption and total emission are determined. This part compares the fuel consumption data for the ship using wing-sail (wing-sail with flap and without flap) as a wind-assisted technology and the original ship. The fuel consumption is calculated based on the engine specification and vessel route selection. To obtain an average net power output of the ship utilizing wing-sail technologies, the net power, fuel consumption, and total fuel savings are calculated by applying the following Equations:

$$A_c = \frac{\pi \times B^2}{4} \quad (3)$$

$$B.P. = \frac{P_{mb} \times L \times A_c \times N}{60000} \quad (4)$$

$$FC = \frac{SFC \times B.P. \times Time}{1000000} \quad (5)$$

$$FS = \frac{SFC \times Avg \text{ net power output} \times Time}{1000000} \quad (6)$$

Where, A_c is cylinder area (m²), B is cylinder bore (m), $B.P.$ is brake power (KW), P_{mb} is brake mean effective pressure (Pa), L is the length of stroke (m), N is RPM of the engine crankshaft, SFC is specific fuel consumption, $Time$ is the total duration of time spent on the individual route in hours, FC is fuel consumption (ton), and FS is fuel saving (ton).

After obtaining the value of fuel consumption, the next step is to determine the total CO₂ emission, which refers to International Maritime Organization (IMO). The total carbon dioxide emission is obtained by applying Eq. (7) according to IMO [24]:

$$CO_2 \text{ emission} = F_{Cnet} \times \text{Emission factor} \quad (7)$$

Where, F_{Cnet} is net fuel consumption per route, and the emission factor is taken as 3.206 for marine diesel oil (MDO) mention by Diaz *et al.*, [25].

2.6 Ship Stability Analysis

In general, a ship should have satisfactory stability while sailing. It is essential that the modern wind-assisted ship should not have a significant influence on its stability in windy condition [9]. Therefore, after analyzing the performance of the wing-sail installed on the tanker, the ship's intact stability must be re-calculated and re-checked for the given criteria.

In order to check the stability criteria of a ship that utilizes wing-sail as wind-assisted technology, there are numerous methods available, which are published by IACS members such as DNV-GL. In this study, the ship stability criteria recommended by Amin *et al.*, [6] and Hu *et al.*, [26] is chosen ship to determine the ship stability while assisted with the wing-sails. The criteria are given below:

- (a) Metacentric height, GM > 0.3 m
- (b) Weather criteria, K ≥ 1

While performing the stability calculations, the Maxsurf software is used to check the stability criteria described by Amin *et al.*, [6] and Hu *et al.*, [26], which is the value of metacentric height (GM) must be greater than 0.3 m. The main output obtained from the calculation of the Maxsurf software is the GZ curve. Then by drawing the tangent to that GZ curve, GM is determined. In this study, the GZ curves for the ship without and with wing-sail are compared, and GMs are calculated to know the influence of installed wing-sail. Since the weight of the wing-sail is crucial to alter the KG of the whole ship and so as to reduce the ship's GZ, in this study the material for the wing-sail is carefully chosen, which is carbon composite because this material is light and robust to use at sea.

The next step is to calculate the weather criteria by considering the following steps, namely the first to calculate the maximum heeling moment recommended by Amin *et al.*, [6] as shown in Eq. (8).

$$M_q = h_2 \times \Delta \quad (8)$$

Where, M_q is the maximum heeling moment (Kg-m), h_2 is gust wind heeling arm (m), and Δ is ship displacement (Kg),

Meanwhile, to calculate the gust wind heeling arm, it is explained in the stability criteria of the DNV-GL rule that $h_2 = 1.5 \times h_1$. In addition, h_1 (wind heeling arm) is calculated according to the DNV-GL rules chapter 15 [27]. Eq. (9) is used in this regard.

$$h_1 = \frac{P \times A \times Z}{1000 \times g \times \Delta} \quad (9)$$

Where, P is pressure, that is taken as 504 N/m² (DNV GL rules Part 03-Chapter 15-Section 01, Point 4.2), A is projected lateral area (m²), g is gravity (m/s²), Δ is ship displacement (Kg), and $Z = d/2 + A/2 * L_{BP}$ (m). Here, d is draft, and L_{BP} is the ship length.

Next, the wind heeling moment (M_f) is calculated, which consists of two parts, namely the moment acting on the ship structure due to the wind (M_{fb}) and the moment acting on the sail due to the wind (M_{fs}). The formula for calculating the wind heeling moment is expressed below:

$$M_f = M_{fb} + M_{fs} \quad (10)$$

To calculate the wind forces and moment acting on the ship, Fujiwara *et al.* wind model [28] is used. This method is used for finding the heeling moment coefficient due to the wind acting on the ship above water part. According to the method, the heeling moment due to wind is calculated by using the following formula:

$$M_{fb} = C_K \times q \times A_L \times H_L \quad (11)$$

Where, C_K is heeling moment coefficient, $C_K = K_1 \sin \Phi + K_2 \sin 2\Phi + K_3 \sin 3\Phi + K_5 \sin 5\Phi$, Φ is the angle of apparent wind acting on ship, $q = 0.5 \times \rho \times V_a^2$, $H_L = A_L/L$ and $\rho = 0.125 \text{ kg m}^3/\text{sec}^4$. The heeling moment due to sail is determined using the following expression:

$$M_{fs} = F_H \times Z_1 \quad (12)$$

Where, F_H is the drift force which is calculated using Eq. (2) and Z_1 is the lever of heeling. Finally, the weather criterion K is calculated for the sail-assisted ships. Hu *et al.*, [26] and Amin *et al.*,

[6] suggested to calculate the K by using the ratio of the maximum heeling moment (M_q) to the wind heeling moment (M_f), as shown in Eq. (13).

$$K = \frac{M_q}{M_f} \tag{13}$$

3. Results and Discussion

3.1 Simulation on ANSYS Fluent

This study utilizes ANSYS 19.2 Fluent platform to measure the lift and drag forces acting on different wing-sails installed on the tanker ship. Due to the limitation of the computational power, only the above draft portion of the ship is considered for single-phase (wind) analysis. Besides, various conditions in the fluid domain, such as different wing-sail types, different wing-sail orientations, and different apparent wind directions, etc., are considered to get the different lift and drag forces acting on each wing-sail. Figure 10 shows the simulation results which illustrates the contours and streamlines when the wind blows at a speed of 4.378 m/s to the ship. This chapter includes only the best result that gives maximum thrust, which is when the wind blows from the beam direction, with wing-sail rotating 45°.

Figure 10 shows the comparison of streamlines of (a) the ship using wing-sail type NACA 4412 with (b), (c), and (d), where flaps are used at different angles. On the other hand, Figure 11 shows the contour picture where it is projected from the top side (Z-axis) to understand the velocity distribution.

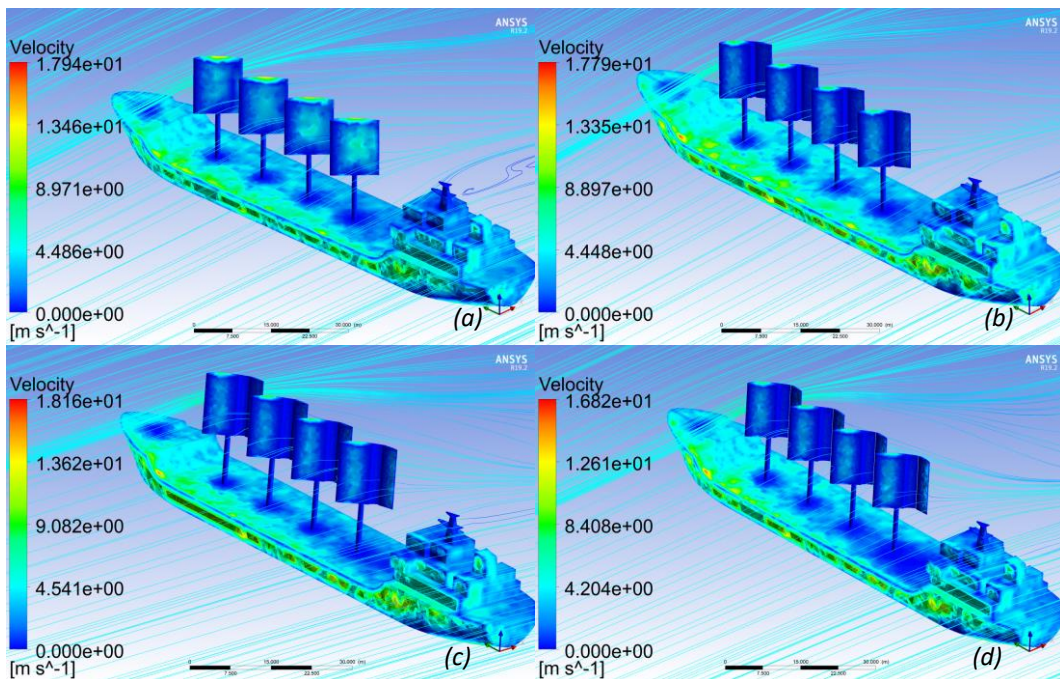


Fig. 5. Streamline 3D view with beam wind (a) Ship with wing-sail NACA-S 4412 (b) Fowler flap at 15°, (c) Fowler flap at 30°, (d) Fowler flap at 45°

The comparisons in Figure 10 and Figure 11 make it clear that the wing-sail with a fowler type flap can capture more wind than the sail alone as the exitance of zero velocity wind zone (Blue zone) beneath the sail is quite large in the case of fowler flap assisted sail. It demonstrates that most of the wind is captured by the sails if it has a flap with an extended projected area. Hence, the fowler flap

can contribute more to adding ship thrust than using only NACA 4412. In addition, Figure 11 (d) shows that sail with a flap at 45° can capture more wind than a sail with a flap at 15° and 30° (Figure 11 (b) and (c)) as it contains a larger extent of zero velocity zone. It is also evident that the fowler flap assisted sail can cause a velocity increase between the wing-sails, and the flap angles can push the wind more effectively than the sail alone. On the other hand, an increase in wind velocity occurs in between the wing-sails which is marked by yellow color. Also, every wing-sail has its own role in which an interaction occurs and results in an additional thrust in other wing-sails. Basically, the angle of attack influences the lift and drag of the wing-sail. In our simulation case, the wind blows from the x-axis direction (beam-wind 90°) with the orientation of the wing-sail 45°, which results in the inward wing-sails having high-pressure distribution than the outward. Additionally, the shape of the wing-sail influences the wind velocity distribution. The inward of wing-sails reduces the wind velocity as it has high pressure on the concave side and generates the lift force towards the Y-axis. However, the outward wing-sail has low-pressure distribution and have a free stream area. Hence, velocity is always higher in the outward than inward.

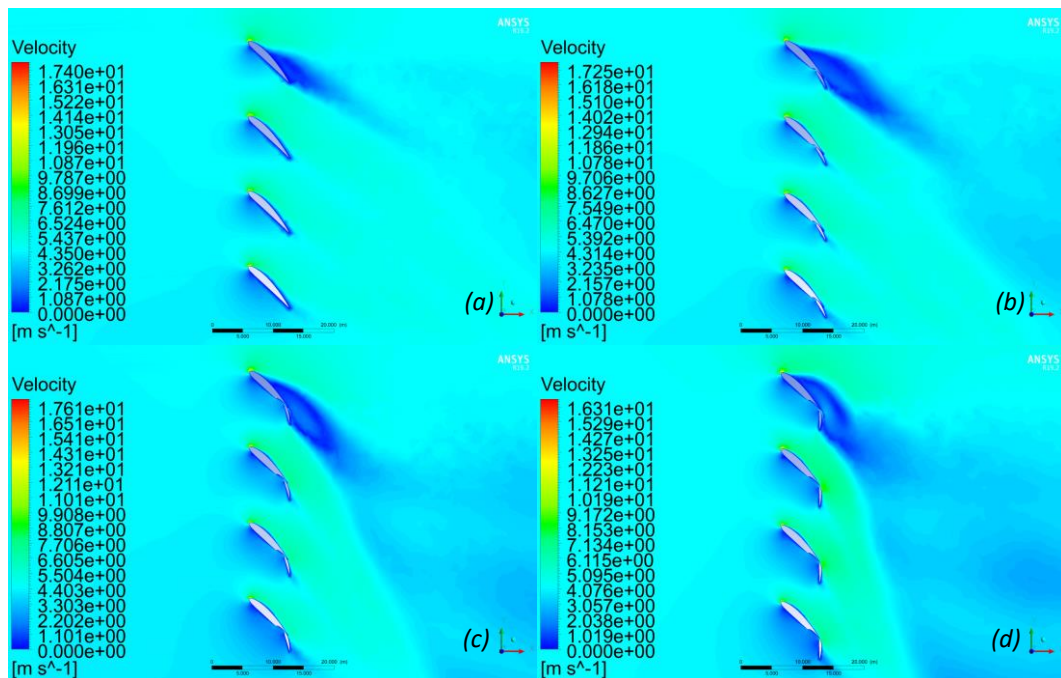


Fig. 6. Velocity contour top view with beam wind (a) Ship with wing-sail NACA-S 4412 (b) Fowler flap at 15°, (c) Fowler flap at 30°, (d) Fowler flap at 45°

3.2 Analysis of Ship Thrust

After the lift and drag forces are calculated using ANSYS Fluent, the thrust is calculated using Eq. (1). The results are plotted for the three different wing-sail orientations, where the apparent wind speed is set at 4.378 m/s. Figures 12, 13, and 14 demonstrate the results for sail orientation 0°, 45°, and 90°, respectively.

All three figures have shown the calculated thrust for both wing-sail and flap assisted wing-sail. Five different apparent wind angles are considered in each figure. Figure 12 demonstrates the result when the wing-sail orientation is set at 0°. Here, the thrust attains its peak when the wind blows from the beam reach direction, i.e., AWA 90°. In that condition, fowler flap assisted sail has been found to be the best one with a flap set at 30°. Fowler type flap at 30° is also found better when the wind blows from close-hauled (45°) to a beam reach (90°) condition. On the other hand, for broad reach

wind (120° and 150°), a significant decrease in the thrust value is observed for both types of sail. The best wing-sail type for broad reach wind is the fowler flap type with a flap set at 45°.

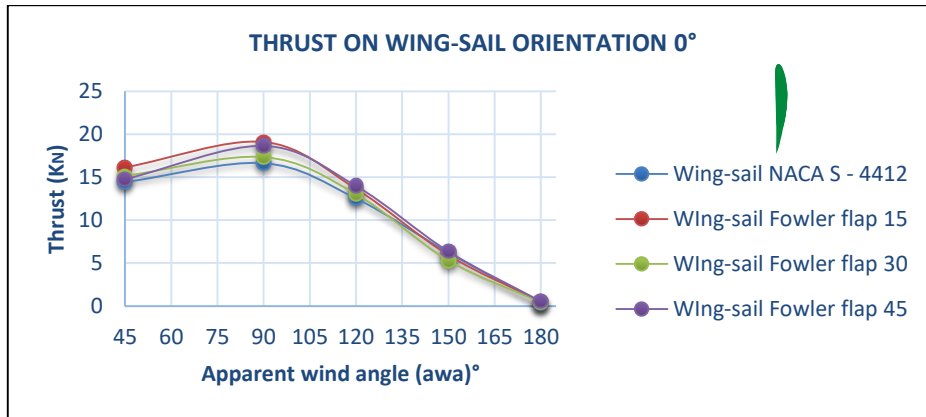


Fig. 7. Thrust acting on wing-sail orientation 0°

Figure 13 shows the results for wing sails set at 45°. Here the highest thrust occurs when the apparent wind direction blows from the beam reach (AWA 90°). Besides, the wing-sail with a fowler flap can help produce additional thrust for the ship than the wing-sail NACA 4412. In addition, the wing-sail with a flap at 45° can produce the maximum thrust. However, when the wind blows from running downwind (180°), the thrust significantly decreases for all other variants of wing-sails.

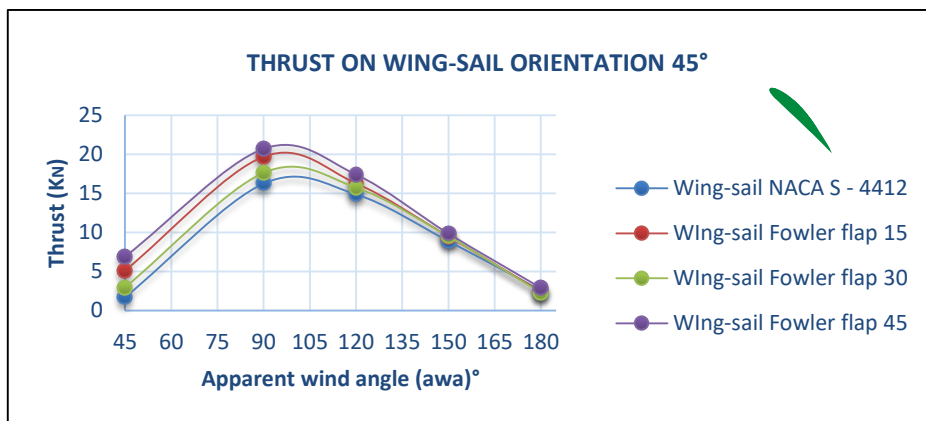


Fig. 13. Thrust acting on wing-sail orientation 45°

Figure 14 shows the thrusts at 90° wing-sail orientation. It has been found that the thrust varies significantly for each apparent wind angle. The best thrust acting on the ship has been found when the apparent wind blows from broad reach (120° and 150°). In addition, the wing-sail with the fowler flap has a significant influence on increasing the thrust of the ship comparing to the NACA S-4412 wing-sail. It can be seen that for every apparent wind angle, the wing-sail with the fowler flap types produces more thrust than the wing-sail NACA S-4412. Especially with fowler flap 45°, the wing-sail can create the best thrust than other wing-sail variants.

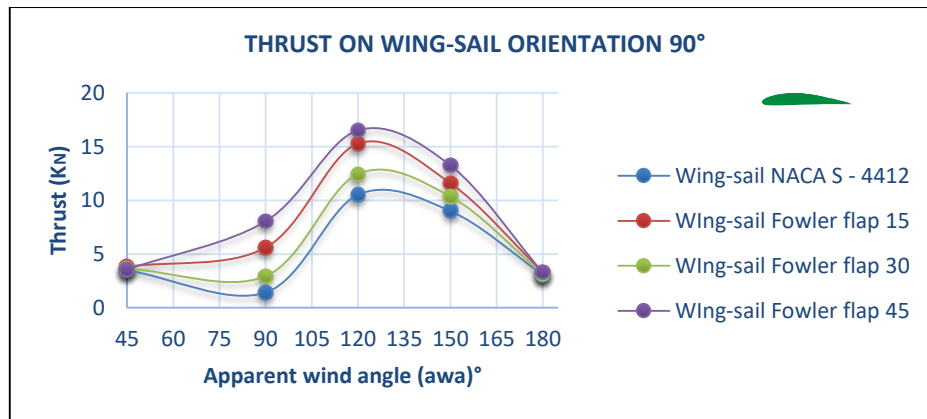


Fig. 14. Thrust acting on wing-sail orientation 90°

In Figure 12 – Figure 14, it is evident that the sail with a flap always gives better results than the sail alone. This is because the flap added an extra dimension for cord length and that inevitably increases the lift and somewhat drag. The results show that sail with flaps performs better regardless of sail orientation and apparent wind angle.

To understand the differences in thrusts for different wing-sail orientations, Figure 15 is considered. It shows the velocity contour of the three different orientations of wing-sail with flap at 30° and 45°. The results are shown for wind that blows from a beam reach. The comparison of the velocity contour demonstrates that for wing orientation 0°, the sail with fowler flap at 30° has captured more wind and thus produces better thrust than the sail with flap at 45°. Also, the interaction of the fowler flap at 30° results in almost zero velocity behind the sail region. Therefore, the fowler flap at 30° has been found to be the most effective in producing additional ship thrust than other variants of the fowler flap. On the other hand, for wing orientation 45° and 90°, the wing with a flap at 45° captures more wind and thus, is the most efficient comparing to other flap options.

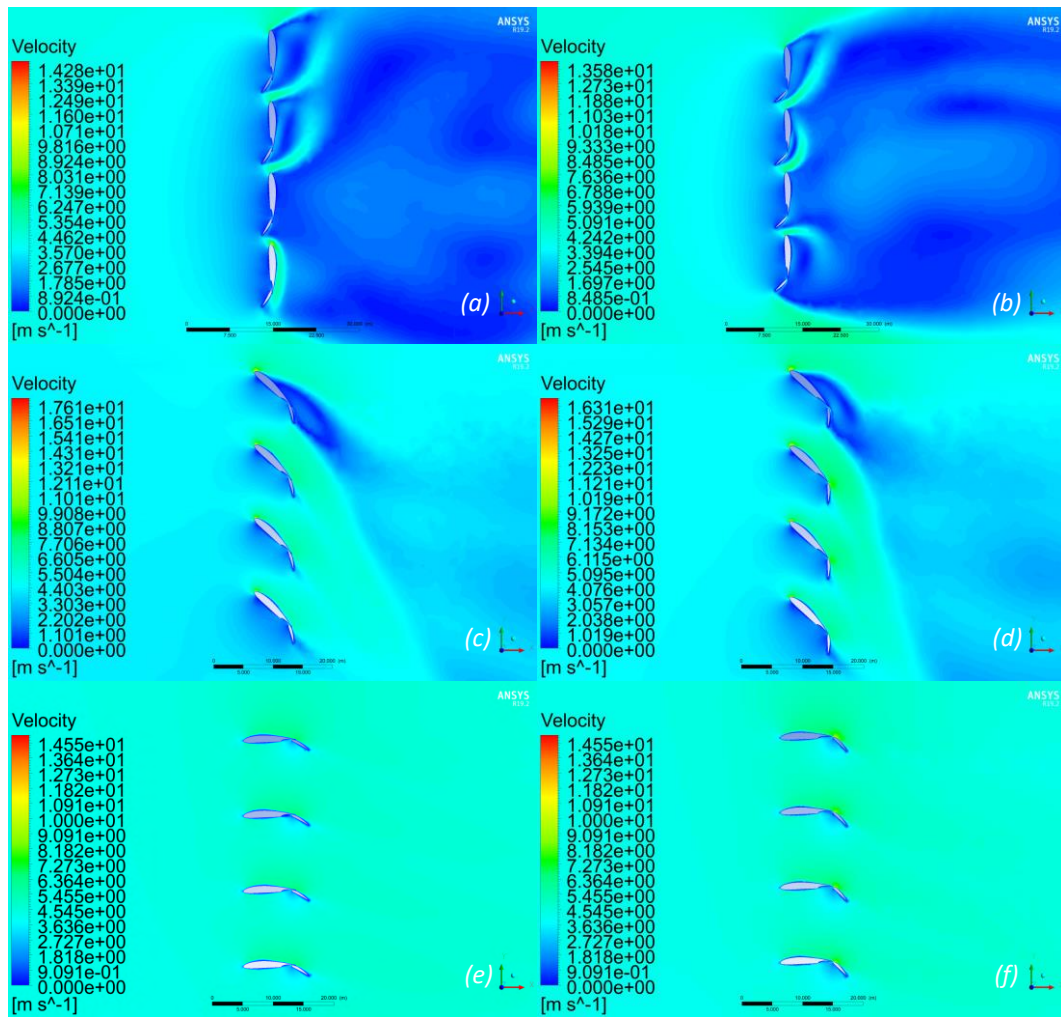


Fig. 15. Top view (Z-axis) of velocity contour (a) fowler flap at 30° and wing-sail orientation 0° , (b) fowler flap at 45° and wing-sail orientation 0° , (c) fowler flap at 30° and wing-sail orientation 45° , (d) fowler flap at 45° and wing-sail orientation 45° , (e) fowler flap at 30° and wing-sail orientation 90° , (f) fowler flap at 45° and wing-sail orientation 90°

According to the basic sailing navigation knowledge, the best sailing condition would be when the apparent wind blows from downwind running (180°), and the wing-sail is set at 90° . However, this did not happen on the 108 m tanker because the superstructure interrupts the wind blowing from the back to the ship (downwind). And also, only one sail can capture the wind adequately, whereas the other sails operate at almost zero velocity. This phenomenon also occurs in other considerations of wing-sail orientations. Thus, it is concluded that when the apparent wind blows from 180° (downwind), the wings-sails of both types cannot generate a good amount of thrust comparing to the other apparent wind angles. To understand the phenomenon, Figure 16 illustrates the streamlines (left) and the contours (right) of the ship operated in downwind condition with wing-sail at 90° .

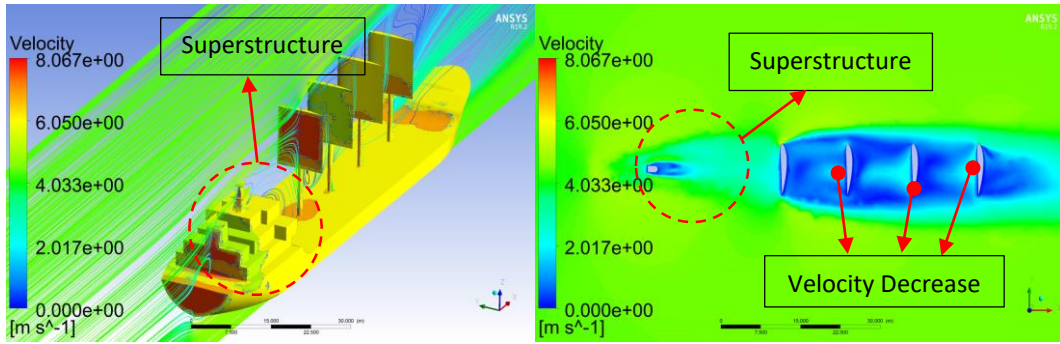


Fig. 8. Streamline (left) and contour (right) ship with wing-sail orientation 90° in downwind condition

3.3 Analysis of Fuel Consumption

After comparing the two types of wing-sail from the perspective of producing additional ship thrust, the next step is to calculate the fuel-saving after the ship utilizes the wing-sail technology. It is possible to do the calculation of required fuel consumptions for an onboard ship engine at a set voyage (in hours). In this study, we have considered the sailing time of 36 hours for the ship to reach its destination. The fuel consumption calculation is shown below.

$$FC = \frac{1 \times 2800 \times 174 \times 36}{0.86 \times 1000000} = 20.39442 \text{ ton (in one trip from Meulabouh to Teluk Bayur)} \quad (14)$$

The fuel-saving is calculated for each different type of wing-sails. The calculated net fuel consumption data for the original ship and the ship with wing-sail of both types are shown in Table 4 and presented as a bar chart in Figure 17.

Referring to Figure 17, it can be seen that the wing-sail plays an effective role in reducing fuel consumption. It shows that the wing-sail with the NACA S-4412 type has an average fuel economy of about 1.87% compared to the original ship without a wing-sail. In addition, the best result while using the wing-sail in terms of fuel economy can be found for fowler flap assisted sail. Based on the calculation, the wing-sail with a fowler flap can save up to an average of 2% with flap at 15° and 2.4% with flap at 45°. Thus, both wing-sail and the flap-assisted wing-sail are effective enough to use for commercial ships to reduce the burning of fossil fuel. Furthermore, the current results are compared and validated with other previously published research works, in which the wind-assisted ship propulsion showed a fuel saving of 1% to 21% [29].

Table 4
 Comparison of ship net fuel consumption

Description	Unit	Value
Ordinary Ship	ton	20.394
Ship w/ Wing-sail NACA S-4412	ton	20.013
Ship w/ Wing-sail Fowler flap in 15°	ton	19.983
Ship w/ Wing-sail Fowler flap in 30°	ton	19.983
Ship w/ Wing-sail Fowler flap in 45°	ton	19.905

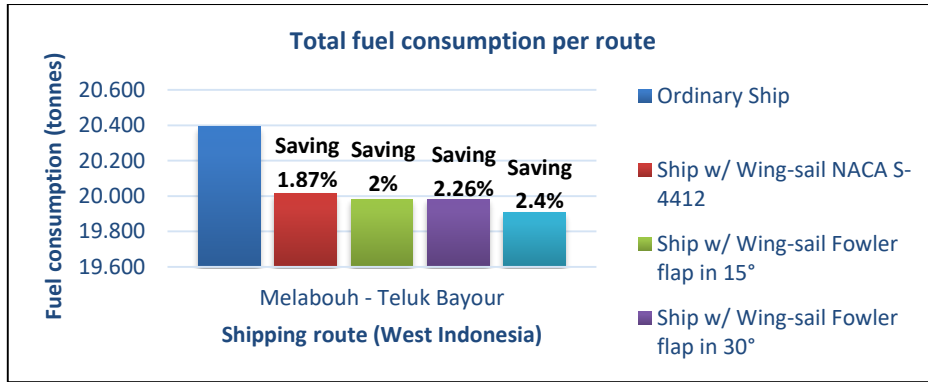


Fig. 9. Total fuel consumption per route

3.4 Analysis of CO2 Emission

This study investigates the carbon dioxide emission and compares the value for an ordinary ship with the one utilizing different variants of wing-sails. The carbon dioxide emission is calculated by multiplying the net fuel consumption with the emission factor of marine diesel oil [25]. Table 5 shows the comparison values, and Figure 18 presents it in form of a bar chart.

Table 5 shows that the carbon dioxide emission by the 108 meters tankers for the prescribed route, which is Meulaboh to Teluk Bayur is 65.385 tons. On the other hand, the ship that uses a wing-sail NACA 4412 results in a decrease of total emissions by 1.2 tons. Also, for the ship that uses a fowler flap, the total emission is reduced by 1.3 up to 1.6 tons per route. The simulation results prove that wing-sail technology can reduce carbon dioxide emissions by 1.87% while using the NACA S-4412 type wing-sail, whereas the fowler flap-assisted wing-sail can reduce emissions by 2% up to 2.4% per shipping route.

Table 5
 Comparison of ship total carbon dioxide emission

Description	Unit	Value
Ordinary Ship	ton	65.385
Ship w/ Wing-sail NACA S-4412	ton	64.163
Ship w/ Wing-sail Fowler flap in 15°	ton	64.065
Ship w/ Wing-sail Fowler flap in 30°	ton	64.066
Ship w/ Wing-sail Fowler flap in 45°	ton	63.815



Fig. 10. Total CO₂ emission per route

3.5 Metacentric Height, GM Calculation

This paper analyses the stability of a sail-assisted ship. The literature review suggested that the stability criteria for a sail-assisted ship should be checked with two essential points. The first one is the initial metacentric height value; GM should be more than 0.3 meters. The other one is the weather criteria; K value must be greater than one [6,26]. Based on the computational results on Maxsurf stability, the GZ curve and the initial metacentric height are calculated for the original and four wing-sail assisted ship. The results are shown in Figure 19 and Table 6. Due to the installation of wing sails, the maximum GZ value is decreased by approximately 4°, from 42.7° to 38.2°. This is due to raising the ship's center of gravity (CG) up by installing the wing-sails. Basically, if the center of gravity increases, the value of the rightening level, GZ decreases. In addition, the initial GM is calculated by taking the slope of the tangent drawn at the GZ curve at zero heel angle. The results show that the GM value after installing the wing-sail is decreased to 1.5 m. This reduced metacentric height is still acceptable to satisfy the stability criteria, which is GM > 0.3 m.

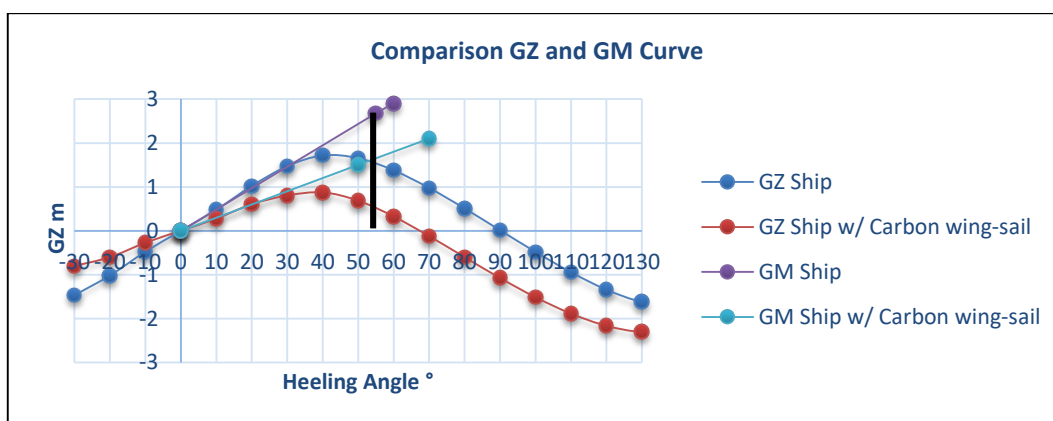


Fig. 11. Comparison of GZ curve and GM value

Table 6
 Initial GM and GZ

Category	Unit	Initial GM	Maximum GZ
Before Wing- sail installation	m	2.679	1.73 at 42.7°
After Wing-sail installation	m	1.504	0.877 at 38.2°

3.6 Weather Criterion, K

This study checks the ship's intact stability by comparing it to the weather criteria. The results are shown in Table 7 – Table 11 for different wing orientations, apparent wind angles, wind velocities, and flap angles.

Table 7 shows the results for the apparent wind angles 45° (close-hauled) with a wing-sail orientation at 0°. The value of K is then calculated for different wind speeds. It has been found that the ship is stable ($K > 1$) with a maximum allowable apparent wind velocity of 5 m/s. In contrast, if the apparent wind speed increases to 6 m/s, the ship becomes unstable ($K < 1$).

Table 7

Weather criterion in AWA close-hauled and wing-sail orientation 0°

AWA	Wing-sail Orientation	AWS (m/s)	NACA 4412 K	Fowler Flap 15° K	Fowler Flap 30° K	Fowler Flap 45° K
45° Close hauled	0°	2	7.21	7.16	7.08	7.51
		4	1.80	1.79	1.77	1.88
		4.378	1.50	1.49	1.48	1.57
		5	1.15	1.15	1.13	1.20
		6	0.80	0.80	0.79	0.83
		8	0.45	0.45	0.44	0.47
		10	0.29	0.29	0.28	0.30

In Table 8, the results are shown for apparent wind angles 90° with a wing-sail orientation at 45°. In this case, the permissible apparent wind velocity is 4.378 m/s. This wind velocity is considered from the real-time weather data while sailing in west Indonesia. Also, based on the calculation, the additional ship thrust that we get from the situation produces the best driving force comparing to other apparent wind angles. However, in the stability analysis, the maximum wind limit that can be handled by this ship for each type of wing-sail is 4.378 m/s.

Table 8

Weather criterion in AWA beam reach and wing-sail orientation 45°

AWA	Wing-sail Orientation	AWS (m/s)	NACA 4412 K	Fowler Flap 15° K	Fowler Flap 30° K	Fowler Flap 45° K
90° Beam wind	45°	2	5.27	5.11	4.91	4.86
		4	1.32	1.28	1.23	1.21
		4.378	1.10	1.07	1.02	1.01
		5	0.84	0.82	0.79	0.78
		6	0.59	0.57	0.55	0.54
		8	0.33	0.32	0.31	0.30
		10	0.21	0.20	0.20	0.19

Table 9 shows the results for apparent wind angles 120° (broad reach wind) with a wing-sail orientation at 90°. For the ship using wing-sail NACA Series 4412, it is considered stable up to an apparent wind velocity of 5 m/s. On the other hand, for other variants, the maximum permissible wind velocity is 4.378 m/s.

Table 9

Weather criterion in AWA broad reach and wing-sail orientation 90°

AWA	Wing-sail Orientation	AWS (m/s)	NACA 4412 K	Fowler Flap 15° K	Fowler Flap 30° K	Fowler Flap 45° K
120° Broad reach wind	90°	2	6.69	6.22	5.70	5.52
		4	1.67	1.55	1.42	1.38
		4.378	1.40	1.30	1.19	1.15
		5	1.07	0.99	0.91	0.88
		6	0.74	0.69	0.63	0.61
		8	0.42	0.39	0.36	0.34
		10	0.27	0.25	0.23	0.22

Table 10 represents the results for an apparent wind angle 150° (broad reach wind) with a wing-sail orientation at 90°. For the ship using wing-sail NACA Series 4412, the threshold occurs at an apparent wind speed of 6 m/s. In addition, the ship utilizing other variants of the fowler flap can be stable up to a wind speed of 5 m/s.

Table 10

Weather criterion in AWA broad reach and wing-sail orientation 90°

AWA	Wing-sail Orientation	AWS (m/s)		Fowler Flap 15°	Fowler Flap 30°	Fowler Flap 45°
		NACA 4412	K	K	K	K
150° Broad reach wind	90°	2	9.85	8.86	8.23	7.46
		4	2.46	2.21	2.06	1.86
		4.378	2.06	1.85	1.72	1.56
		5	1.58	1.42	1.32	1.19
		6	1.09	0.98	0.91	0.83
		8	0.62	0.55	0.51	0.47
		10	0.39	0.35	0.33	0.30

Finally, Table 11 shows the results for apparent wind angles 180° (downwind running) with a wing-sail orientation at 90°. Here, each variant of wing-sail has almost the same K value. The ship using different wing-sail variants can handle the apparent wind up to 8 m/s without sacrificing its stability. However, when the apparent wind speed has increased to 10 m/s, the ship becomes unstable.

Table 11

Weather criterion in AWA downwind and wing-sail orientation 90°

AWA	Wing-sail Orientation	AWS (m/s)		Fowler Flap 15°	Fowler Flap 30°	Fowler Flap 45°
		NACA 4412	K	K	K	K
180° Downwind running	90°	2	19.82	19.57	18.69	18.50
		4	4.96	4.89	4.67	4.63
		4.378	4.14	4.09	3.90	3.86
		5	3.17	3.13	2.99	2.96
		6	2.20	2.17	2.08	2.06
		8	1.24	1.22	1.17	1.16
		10	0.79	0.78	0.75	0.74

From the aforementioned results, it is concluded that the ship has always possessed a satisfactory level of stability irrespective of different sail orientations and flap variations for an apparent wind speed of 4.378 m/s. However, in some situations, if the apparent wind speed is above 4.378 m/s, the ship can experience instability depending on sail and flap orientations. The wing-sail orientation plays a viable role in maintaining the ship's stability. Thus, the optimal wing-sail orientation must be decided depending on apparent wind velocities and apparent wind angles to keep the vessel stable in all weather conditions.

4. Conclusions

In this research, the impact of wind-assisted technology has been analyzed for producing extra thrust and the possible effect on the stability of a commercial ship. A tanker ship is chosen in this regard that utilizes four wing-sails with and without flap to harness the wind energy. Different sail orientations, apparent wind speeds, and apparent wind angles are tested for this ship to calculate

the thrust in each different combination. ANSYS Fluent platform is used for the CFD simulation, and results are included in the paper. Based on additional thrust produced by the wing sails, fuel-saving and reduced CO₂ emission are also calculated. It is concluded that the ship that utilizes wing-sail can produce additional thrust compared to the actual ship, resulting in a saving of approximately 2% of fuel for a pre-selected voyage. In addition, an increase in the saving fuel is possible by including a fowler flap in wing-sail which can capture more wind due to having extended surface area. It has been found that the fowler flap assisted wing-sail can save up to 2.4% of the fuel and the same percentage of reduction of carbon dioxide emission. While comparing the different variants of wing-sail types and different orientations, a ship using sail with fowler-flap with an orientation at 45° has been found to be the best choice which can produce the maximum amount of thrust for this tanker ship.

Ship using wing-sail can have an adverse effect on its stability at high wind speeds. Therefore, it is crucial to set an optimum orientation of the wing-sail to get the best thrust without compromising its stability. It has been found that in the downwind condition, the ship can accept 8 m/s speed without compromising the weather criteria. However, the sails can produce a minimum amount of thrust in the same condition.

As future work, more wing-sail orientations need to be investigated to check the stability criteria. The variation of the distance in between the wing-sails also needs to be examined. In addition, variations of the shape of the wing-sail could also be a part of future work.

Acknowledgement

This research was supported by Research University Grant—UTM ER [Vot Number: Q.J130000.3851.19J33] initiated by UTM.

References

- [1] Yau, P. S., S. C. Lee, James J. Corbett, Chengfeng Wang, Y. Cheng, and K. F. Ho. "Estimation of exhaust emission from ocean-going vessels in Hong Kong." *Science of the total environment* 431 (2012): 299-306. <https://doi.org/10.1016/j.scitotenv.2012.03.092>.
- [2] Chang, Ching-Chih, and Po-Chien Huang. "Carbon allowance allocation in the shipping industry under EEDI and non-EEDI." *Science of The Total Environment* 678 (2019): 341-350. <https://doi.org/10.1016/j.scitotenv.2019.04.215>.
- [3] Shoib, Abdul Rashid, Djamal Hissein Didane, Akmal Nizam Mohammed, Kamil Abdullah, and Mas Fawzi Mohd Ali. "Technical Assessment of Wind Energy Potentiality in Malaysia Using Weibull Distribution Function." *Journal of Advanced Research in Fluid Mechanics and Thermal Sciences* 86, no. 1 (2021): 1-13. <https://doi.org/10.37934/arfmts.86.1.113>
- [4] Elkaim, Gabriel Hugh, and CO Lee Boyce Jr. "Experimental aerodynamic performance of a self-trimming wing-sail for autonomous surface vehicles." *IFAC Proceedings Volumes* 40, no. 17 (2007): 271-276. <https://doi.org/10.3182/20070919-3-hr-3904.00048>.
- [5] Silva, Manuel F., Anna Friebe, Benedita Malheiro, Pedro Guedes, Paulo Ferreira, and Matias Waller. "Rigid wing sailboats: A state of the art survey." *Ocean Engineering* 187 (2019): 106150. <https://doi.org/10.1016/j.oceaneng.2019.106150>.
- [6] Amin, Osman Md, Md Daluar Hussain, Md Shahnewaz Tuhin, and Md Shahariar Kabir. "A CONCEPTUAL ANALYSIS OF GREEN SHIP TECHNOLOGY USING WIND PROPULSION SYSTEM TO REDUCE FUEL CONSUMPTION AND EMISSION.", In *Conference on Ship and Offshore Technology ICSOT 2017*. (2017).
- [7] Li, Qiao, Yasunori Nihei, Takuji Nakashima, and Yoshiho Ikeda. "A study on the performance of cascade hard sails and sail-equipped vessels." *Ocean Engineering* 98 (2015): 23-31. <https://doi.org/10.1016/j.oceaneng.2015.02.005>.
- [8] Ma, Yong, Huaxiong Bi, Mengqi Hu, Yuanzhou Zheng, and Langxiong Gan. "Hard sail optimization and energy efficiency enhancement for sail-assisted vessel." *Ocean Engineering* 173 (2019): 687-699. <https://doi.org/10.1016/j.oceaneng.2019.01.026>.
- [9] Fujiwara, Toshifumi, Grant E. Hearn, Fumitoshi Kitamura, Michio Ueno, and Yoshimasa Minami. "Steady sailing performance of a hybrid-sail assisted bulk carrier." *Journal of marine science and technology* 10, no. 3 (2005): 131-146. <https://doi.org/10.1007/s00773-004-0189-3>.
- [10] Skybrary. "Flaps." July 27, 2017.

- [11] Wang, Wenhui, Peiqing Liu, Yun Tian, and Qiulin Qu. "Numerical study of the aerodynamic characteristics of high-lift droop nose with the deflection of fowler flap and spoiler." *Aerospace Science and Technology* 48 (2016): 75-85. <https://doi.org/10.1016/j.ast.2015.10.024>.
- [12] Cutler, Colin. "How The 4 Types Of Aircraft Flaps Work." *Boldmethod*. May 05, 2018.
- [13] Wikipedia. "Computational fluid dynamics." Accessed January 12, 2021.
- [14] Mechanical Solutions, Inc. "Computational fluid dynamics." Accessed December 25, 2020.
- [15] Autodesk. "SST K-Omega Turbulence Models." August 28, 2018.
- [16] Zhao, Dan, Nuomin Han, Ernest Goh, John Cater, and Arne Reinecke. "Chapter 2 - 3D-printed miniature Savonius wind harvester." in *Wind Turbines and Aerodynamics Energy Harvesters*, (2019): 21-165. <https://doi.org/10.1016/B978-0-12-817135-6.00002-8>.
- [17] Malvè, Mauro, Gérard Finet, Manuel Lagache, Ricardo Coppel, Roderic I. Pettigrew, and Jacques Ohayon. (2021). "Chapter 10 - Hemodynamic disturbance due to serial stenosis in human coronary bifurcations: a computational fluid dynamics study, in Biomechanics of Coronary Atherosclerotic Plaque." *Volume 4 in Biomechanics of Living Organs*, (2021): 225-250. <https://doi.org/10.1016/B978-0-12-817195-0.00010-X>.
- [18] PT. Batamec Shipyard. "Latest shipbuilding project, Merchant vessel, Transko Yudhistira." Accessed January 10, 2021.
- [19] Rodrigue, Jean-Paul. "Types of maritime routes." *Transportgeography*. Accessed January 10, 2021.
- [20] Werner, Jeff. "How to sail: What are the different points of sail." *Allatsea*. October 24, 2020.
- [21] Wasserman, Shawn. "Choosing the right turbulence model for your CFD simulation - Turbulence model definitions, strengths, weaknesses and best practices for your CFD simulation." *Engineering*. November 22, 2016.
- [22] Heteyi, Csaba, Ildikó Molnár, and Ferenc Szlivka. "Comparing different CFD software with NACA 2412 airfoil." *Progress in Agricultural Engineering Sciences* 16, no. 1 (2020): 25-40. <https://doi.org/10.1556/446.2020.00004>.
- [23] Li, Dongqin, Yili Zhang, Peng Li, Jingjing Dai, and Guohuan Li. "Aerodynamic Performance of a New Double-Flap Wing Sail." *Polish Maritime Research* 26, (2019): 61-68. <https://doi.org/10.2478/pomr-2019-0067>.
- [24] International Maritime Organization. "Energy efficiency measures." Accessed May 18, 2020.
- [25] Díaz-Ruiz-Navamuel, Emma, Andrés Ortega Piris, and Carlos A. Pérez-Labajos. "Reduction in CO2 emissions in RoRo/Pax ports equipped with automatic mooring systems." *Environmental Pollution* 241 (2018): 879-886. <https://doi.org/10.1016/j.envpol.2018.06.014>.
- [26] Hu, Yihuai, Juanjuan Tang, Shuye Xue, and Shewen Liu. "Stability criterion and its calculation for sail-assisted ship." *International Journal of Naval Architecture and Ocean Engineering* 7, no. 1 (2015): 1-9. <https://doi.org/10.2478/ijnaoe-2015-0001>.
- [27] DNV GL. *Part 3 Hull Chapter 15 - Stability, Rules For Classification Ships*, (2017): 10-11.
- [28] Fujiwara, Toshifumi, Michio Ueno, and Tadashi Nimura. "Estimation of wind forces and moments acting on ships." *Journal of the Society of Naval Architects of Japan* 1998, no. 183 (1998): 77-90. <https://doi.org/10.2534/ijnaoe1968.1998.77>.
- [29] Lu, Ruihua, and Jonas W. Ringsberg. "Ship energy performance study of three wind-assisted ship propulsion technologies including a parametric study of the Flettner rotor technology." *Ships and Offshore Structures* 15, no. 3 (2020): 249-258. <https://doi.org/10.1080/17445302.2019.1612544>.